NeuroImage 328 (2026) 121797

Contents lists available at ScienceDirect

NeuroImage

journal homepage: www.elsevier.com/locate/ynimg

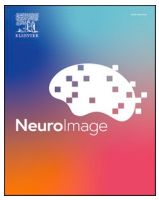

Stress-induced takotsubo syndrome: dynamic changes in regional cerebral metabolism revealed by quantitative PET imaging

Alejandro Ariza-Carrasco [a,b,1], Thulaciga Yoganathan [c,1], María Alonso de Leciñana [d], Thomas Viel [e,f], Nidaa Mikail [e,g,h,i,j], Joaquin L. Herraiz [a,b], Jose M. Udias [a,b], Paula Ibáñez [a,b], Bertrand Tavitian [e,f,2,*], Mailyn Pérez-Liva [k,2,*]

[a] Nuclear Physics Group and IPARCOS, Department of Structure of Matter, Thermal Physics and Electronics, CEI Moncloa, Universidad Complutense de Madrid, 28040 Madrid, Spain
[b] Departamento de Estructura de la Materia, Física Térmica y Electrónica, Facultad de Ciencias Físicas, Universidad Complutense de Madrid (UCM); IdISSC, España
[c] Calico Life Sciences LLC, 1170 Veterans Blvd, South San Francisco, CA 94080, USA
[d] Department of Neurology and Stroke Centre, Neurological Sciences and Cerebrovascular Research Laboratory, Neurology and Cerebrovascular Disease Group, Neuroscience Area Hospital La Paz Institute for Health Research-IdiPAZ (La Paz University Hospital, Universidad Autónoma de Madrid), Madrid, Spain
[e] Université Paris Cité, Inserm, PARCC, F-75015 Paris, France
[f] Radiology Department, AP-HP, European Hospital Georges-Pompidou, F-75015 Paris, France
[g] Nuclear Medicine Department, AP-HP, European Hospital Georges-Pompidou, DMU IMAGINA, F-75015 Paris, France
[h] Center for Molecular Cardiology, University of Zurich, 8952 Schlieren, Switzerland
[i] Department of Nuclear Medicine, Cantonal Hospital Baden, Partner Hospital for Research and Teaching of the Medical Faculty of the University of Zurich, Baden, 5404, Switzerland
[j] Department of Nuclear Medicine, University Hospital Zurich, Zurich, Switzerland
[k] Instituto de Tecnologías Físicas y de la Información "Leonardo Torres Quevedo" (ITEFI-CSIC), C/Serrano, 144, Madrid, Spain

ARTICLE INFO

Keywords:
Quantitative PET imaging
2-deoxy-2-[^{18}F]fluoro-D-glucose (FDG)
Takotsubo syndrome
Regional cerebral metabolism
Acute catecholaminergic stress

ABSTRACT

Stress significantly contributes to cardiovascular diseases such as Takotsubo syndrome (TTS), which mimics an acute coronary syndrome without coronary obstruction. TTS is triggered by surgery, trauma, and emergency treatments in patients, and is reproduced in animal models by a catecholamine surge that impacts cardiac sympathetic innervation. The action of catecholamines on energy metabolism is well documented in the heart, less so in the brain. We investigated the effects of acute catecholaminergic stress on regional cerebral glucose metabolism and interregional metabolic organization in a TTS rat model using FDG-PET and quantitative two-tissue compartment modeling. Adult female rats received a single intraperitoneal injection of isoprenaline (ISO) (50 mg/kg). Dynamic FDG-PET imaging was performed at baseline, 2 hours (acute phase), and 7 days (recovery phase) post-injection. Kinetic parameters, namely glucose inflow (K1) and glucose phosphorylation (k3), were quantified in 58 brain regions. Interregional metabolic coordination, defined as statistically significant linear correlations between regional kinetic parameters, was assessed across functional brain areas. During the acute phase, the catecholaminergic surge induced widespread reductions in glucose inflow and regional decreases in phosphorylation, particularly in the limbic and sensorimotor areas. During the recovery phase, most regions remained below baseline. Metabolic coordination increased for glucose inflow in both phases but declined for phosphorylation, especially during recovery, indicating a disruption of metabolic synchronization. Persistent changes in brain metabolism imply that mid-to-long-term changes in regional cerebral metabolism may contribute to long-term TTS consequences.

* Corresponding authors.
E-mail addresses: bertrand.tavitian@inserm.fr (B. Tavitian), mailyn.perez.liva@csic.es (M. Pérez-Liva).
[1] both authors contributed equally and share the first authorship
[2] these authors share the corresponding authorship

https://doi.org/10.1016/j.neuroimage.2026.121797
Received 29 July 2025; Received in revised form 14 January 2026; Accepted 9 February 2026
Available online 10 February 2026

1. Introduction

While physiological responses to stress are a built-in behavior conferring a survival advantage, excessive mental stress can induce serious cardiac conditions (Arri et al., 2016). As early as the 18th century, the exacerbation of emotions was linked to cardiac conditions such as *angina pectoris* (Heberden, 1802). Over the years, numerous studies have shown that acute and chronic stress can trigger coronary artery disease, stroke, atrial fibrillation, and other cardiovascular conditions. Chronic stress also impedes recovery and accelerates disease progression (Kivimäki and Kawachi, 2015; Dragano et al., 2017; Kivimäki and Steptoe, 2018), through prolonged systemic inflammation, increased coagulation, blood clot formation, heightening the risk of plaque rupture and subsequent ischemic cardiovascular events (Carey et al., 2014; Kivimäki et al., 2017).

A clinical entity triggered by acute stress known as Takotsubo syndrome (TTS; see Table 1 for a complete list of abbreviations used throughout the manuscript) was recognized in the 1990s in Japan (Templin et al., 2015). TTS presents as an acute coronary syndrome following intense stress, but without obstructive coronary artery disease that predominantly affects women (over 90 % of reported cases) (Gianni et al., 2006). During the acute symptomatic phase, the TTS heart often shows an atypical shape with apical ballooning (a "tako-tsubo", octopus fishing pot), but coronary angiography shows no sign of arterial obstruction. Acute TTS may be fatal, though most often cardiac symptoms resolve in a few days without noticeable sequelae. However, longitudinal multicenter studies of this rare syndrome have shown excess mid- to long-term mortality rates similar to those of ST-segment elevation acute coronary syndrome, and recurrence rates of approximately 4 % per year (Stiermaier et al., 2016; Ghadri et al., 2018; Scally et al., 2018; Pelliccia et al., 2019; Wang et al., 2020; Looi et al., 2022; Singh et al., 2022; Fernández-Cordón et al., 2023), suggesting that acute stress induces a silent or difficult-to-detect, slow continuous degradation of the cardiac function.

The exact mechanism of TTS is still a matter of discussion (Madias, 2024; 2025), but there is a consensus about the cardiac response to acute mental stress. In response to perceived threats, sensory signals are processed by the brain's limbic system, cerebral cortex, and hypothalamus, activating two principal neurohormonal pathways: the hypothalamic-pituitary-adrenal (HPA) axis and the sympathetic-adrenal-medullary (SAM) system (Sarmiento et al., 2024). The HPA axis triggers the release of cortisol, mediating prolonged stress responses by modulating metabolism and immune functions. Concurrently, the SAM system initiates rapid responses by increasing heart rate and vasoconstriction, preparing the body for immediate action. These systems are interconnected; glucocorticoids from the HPA axis enhance catecholamine synthesis in the SAM system, demonstrating the intricate feedback loops that regulate stress responses (Herman et al., 2016). Catecholaminergic surge is the prominent mechanism inducing the acute signs of TTS, as shown by reports of iatrogenic induction of TTS by isoprenaline (ISO) administration (Collen et al., 2008; Redfors et al., 2014; Satyavolu et al., 2022), and by the prevalence of TTS in pheochromocytoma patients (Shams, 2016 ; Xu et al., 2024), and after different types of physical stress, e.g. surgery or trauma (Nyman et al., 2019; Laghlam et al., 2023). Accordingly, animal models based on acute ISO administration accurately recapitulate the TTS syndrome, including short- and long-term cardiac dysfunction (Hayashi et al., 2023; Yoganathan et al., 2023). It thus appears that a catecholaminergic surge leads to similar cardiac TTS symptoms via three different routes: mental/emotional, physical, and pharmacological stressors.

Considering that (i) TTS mechanisms remain incompletely understood (Ghadri et al., 2018; Wang et al., 2020; Madias, 2024), and (ii) emerging evidence suggests a strong link between the central nervous system (CNS) and the heart during the response to acute stress in TTS (Silva et al., 2019; Khan et al., 2023), it is of interest to analyze the CNS response to a catecholamine storm to better understand how a single acute stress event leads to long-lasting cardiac dysfunction. A better understanding of the response of the brain to the catecholamine storm may also unveil crucial factors contributing to the persistent vulnerabilities observed in TTS patients and contribute to the search for preventive interventions. Catecholamines (epinephrine and norepinephrine) initiate a cascade of adaptive and maladaptive responses aimed at managing stressors. The "fight or flight" mechanism, first described by Cannon and De La Paz, and Selye's "general adaptation syndrome" illustrate how the body coordinates complex systems to maintain physiological stability under stress (Cannon, 1915; Selye, 1950).

Patients with TTS often exhibit altered brain activity in regions involved in stress and autonomic regulation, such as the amygdala, hippocampus, and prefrontal cortex, implicating CNS involvement in TTS onset and severity (Silva et al., 2019; Radfar et al., 2021; Khan et al., 2023). TTS involving neurological disorders is associated with worse long-term outcomes (Fernández-Cordón et al., 2023). Additionally, a history of neurological disorders (including cerebrovascular events, neurodegenerative diseases, and epilepsy) predicts in-hospital complications during TTS admissions (Santoro et al., 2019; 2024). Recent research has highlighted the neurological dimensions of TTS through functional magnetic resonance imaging (fMRI) studies, revealing altered functional connectivity within key brain structures governing emotions, memory, and autonomic function in TTS patients (Silva et al., 2019; Templin et al., 2019; Dichtl et al., 2020; Khan et al., 2023). Notably, these changes persist beyond the acute phase, emphasizing implication of the CNS in the syndrome. Furthermore, as a highly energy-dependent organ, the brain relies on a constant supply and utilization of glucose (Dienel, 2019). A sudden and massive influx of catecholamines could trigger widespread or region-specific alterations in cerebral glucose metabolism, potentially affecting autonomic outflow and stress modulation, thereby contributing to both the acute cardiac dysfunction and the sustained risks associated with TTS.

Molecular imaging using 2-deoxy-2-[^{18}F]fluoro-D-glucose positron emission tomography (FDG-PET) to assess cerebral glucose metabolism has not been used outside of preclinical research in TTS (Wang et al., 2022). In our previous work using a rodent model, we demonstrated that a single catecholamine challenge induces TTS-like cardiomyopathy,

Table 1
Table of abbreviations used and their corresponding definitions.

Abbreviations	Definitions
TTS	Takotsubo syndrome
STEMI	ST-segment elevation myocardial infarction
HPA axis	Hypothalamic–pituitary–adrenal axis
SAM	Sympathetic–adrenal–medullary system
ISO	Isoprenaline (Isoproterenol hydrochloride)
CNS	Central nervous system
fMRI	Functional magnetic resonance imaging.
MRI	Magnetic resonance imaging
FDG	2-deoxy-2-[^{18}F]fluoro-D-glucose
PET	Positron emission tomography
FDG-PET	2-deoxy-2-[^{18}F]fluoro-D-glucose positron emission tomography.
K1	Glucose inflow (Unit: ml/ccm/min).
k3	Glucose phosphorylation (Unit: min^{-1})
post-ISO	Post-injection of isoprenaline
ECG	Electrocardiogram
LV	Left ventricular
GLUT1	Glucose transporter type 1
GLUT4	Glucose transporter type 4
BNP	B-type natriuretic peptide
CT	Computed tomography
3D-OSEM	Three-dimensional Ordered-Subsets Expectation–Maximization
PMOD	PMOD software
TACs	Time-activity curves
AIF	Arterial input function
IDIF	Image-derived input function
ROI	Region of interest
CBF	Cerebral blood flow

accompanied by significant changes in blood biomarkers and cardiac imaging and provided a robust TTS-model (Yoganathan et al., 2023). Long-term monitoring revealed that catecholamine-induced cardiomyopathy leads to irreversible cardiac alterations, including metabolic reprogramming and progressive fibrosis. Controlled TTS-like animal models provide a unique opportunity to investigate these metabolic changes, and standardized catecholamine administration allows reproducible stress responses.

In the present study, we focus on the immediate and delayed effects of acute catecholaminergic stress on regional cerebral metabolism, using FDG-PET imaging with quantitative two-tissue compartmental modeling in a TTS animal model. We quantify the kinetics of FDG inflow (K1) and phosphorylation (k3) to determine regional metabolic alterations within specific brain regions, including areas involved in autonomic regulation and emotional processing. We complement the regional analysis with a metabolic correlation analysis based on interregional associations of kinetic parameters and explore brain-wide metabolic organization during disease progression.

2. Methods

2.1. Animal model

The study was approved by the Animal Ethics Committee of the French Ministry of Research (approval number: 19-064) and followed Directive 2010/63/EU of the European Parliament regarding the protection of animals used for scientific purposes. Because TTS affects mostly female patients (Gianni et al., 2006), the study was conducted on

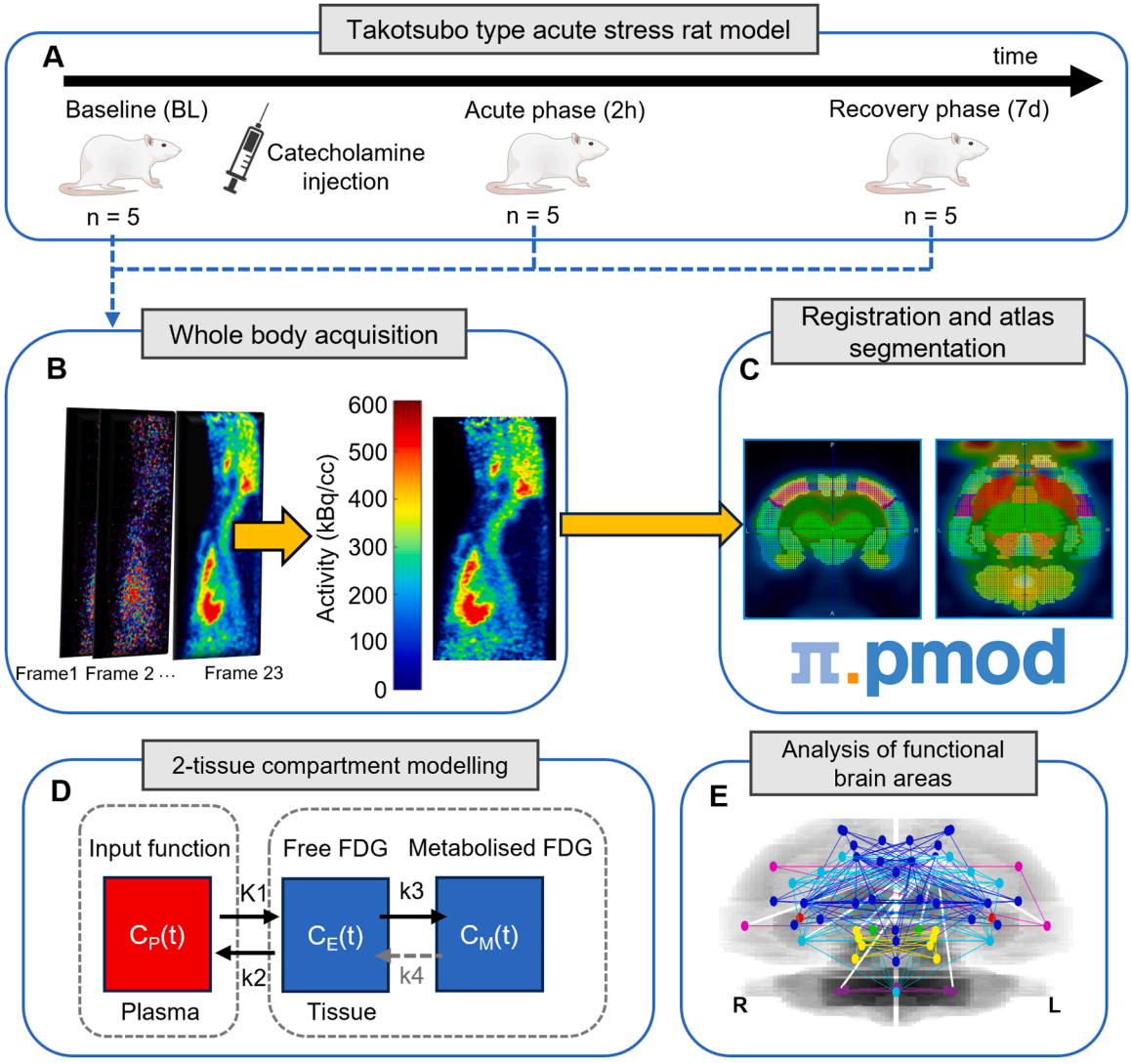

Fig. 1. Experimental design, imaging protocol, and data analysis workflow. A) Takotsubo syndrome (TTS) was induced by a single intraperitoneal injection of isoprenaline (ISO) (50 mg/kg) in adult female rats, to induce an acute catecholamine surge. In vivo imaging was performed at three time points: baseline (BL), 2 hours post-injection (acute phase, characterized by a transient left ventricular dysfunction), and 7 days post-injection (recovery phase, with functional improvement). A total of 15 animals were used (n = 5 per time point). B) Dynamic FDG-PET imaging was acquired over 30 minutes in 23 consecutive time frames. C) Brain FDG-PET was processed using PMOD software (version 3.7, PMOD Technologies LLC, Zurich), including elastic registration to the W. Schiffer rat brain atlas (Schiffer et al., 2006) for segmentation into 58 cerebral regions. D) A two-tissue compartment model was applied to estimate kinetic constants: K1 (glucose inflow) and k3 (glucose phosphorylation). E) Metabolic correlation analysis assessed coordinated metabolic responses across brain areas during TTS progression. Pearson's correlation coefficients were calculated between all region pairs using K1 and k3 values. Significant correlations were defined as $|r| \geq 0.9$ and $p \leq 0.05$. Mass centroids of the volumes of all brain regions were projected onto 2D planes overlaid on a grey-scale horizontal projection of the W. Schiffer rat brain atlas. Significant correlations between regions are represented as distinct colored lines for the functional brain areas: parietal (red) ■ retrosplenial (green) ■, limbic (blue) ■, sensorimotor (cyan) ■, audiovestibular (magenta) ■, midbrain (yellow) ■, and cerebellar (purple) ■. White lines indicate significant correlations between regions from different functional brain areas.

female healthy 12-week-old Wistar rats (Janvier, Le Genest-St-Isle, France). The rats were housed in monitored conditions at 25°C with humidity between 45 % and 85 %, provided *ad libitum* access to food (Lignocel) and water, and maintained on a 12-hour light-dark cycle. All experiments were initiated between 8:30 and 9:30 a.m. and were consistently conducted by the same experienced personnel to ensure uniformity in experimental procedures.

Acute stress TTS was induced using a single intraperitoneal injection of 50 mg/kg ISO (Isoproterenol hydrochloride, Sigma-Aldrich, Germany). The effects of the catecholamine surge observed in TTS patients (Khan et al., 2023) were controlled at baseline, 2 hours (acute phase characterized by a transient left ventricular (LV) dysfunction), and 7 days (recovery phase) post-ISO (Fig. 1A) as in Yoganathan et al. (2023). A set of n=5 animals was studied per time point, totaling 15 rats. We used different animals at each time point to avoid the risk of carryover effects or cumulative stress responses, in individual rats. At the end point of the study, the rats were euthanized via intraperitoneal injection of Pentobarbital (100 mg/kg, Euthasol, LE VET, Oudewater, Netherlands). A full characterization and validation of this pharmacologically induced TTS-like rat model were previously reported by our group (Yoganathan et al., 2023), demonstrating its ability to recapitulate key clinical features of TTS. Briefly, during the acute phase, all rats exhibited physical signs of a stress-induced cardiomyopathy, including electrocardiogram (ECG) abnormalities, decreased blood pressure, and heterogeneous regional LV wall-motion abnormalities (LV apex vs. LV base). This acute metabolic response was accompanied by a global rise in myocardial FDG uptake driven by increased K1 and increased glucose transporter type 1 (GLUT1) expression; notably, the insulin-dependent glucose transporter type 4 (GLUT4) remained unchanged at the acute phase, consistent with a state resembling myocardial glucose intolerance. Most functional signs and plasma biomarkers (except B-type natriuretic peptide (BNP)) had returned to normal by the recovery phase (7d post-ISO). However, persistent metabolic and structural sequelae remained (including elevated FDG uptake with activation of anabolic glucose pathways (hexosamine biosynthetic pathway, and polyol pathway), an increased phosphorylation rate, high GLUT1/GLUT4 expression, and irreversible apical tissue and vascular remodeling (diffuse fibrosis, elevated vascular markers)), thus providing a mechanistic link to the irreversible apical remodeling observed clinically.

2.2. Imaging protocol

Dynamic PET imaging (Fig. 1B) of cerebral metabolism was obtained in non-fasted rats anesthetized with 2.7 ± 0.6 % isoflurane in medical air. To ensure the reliability of our FDG-PET results and allow for a rigorous comparison between post-ISO groups, we imposed careful and continuous monitoring of rat physiological conditions. The isoflurane anesthesia rate and heating system were adjusted continuously throughout the imaging session to ensure that the respiratory rate and the body temperature were stable and comparable across all experimental groups (including baseline) (see Supplementary Data 1). Body weight and blood glucose levels were measured before and 2 hours after ISO injection. Each rat received an intravenous injection of 32.2 ± 1.8 MBq of FDG in 0.4 mL saline. To enable PET attenuation correction, whole-body images were acquired via computed tomography (CT) scan using a nanoScan PET-CT scanner (Mediso Medical Imaging Systems, Hungary). PET data were collected in list mode and binned using a 5 ns time window, with a 400-600 keV energy window and a 1:5 coincidence mode. Data was reconstructed using the Tera-Tomo reconstruction software (Three-dimensional Ordered-Subsets Expectation–Maximization (3D-OSEM) based manufactured customized reconstruction algorithm) with expectation maximization iterations, scatter, and attenuation correction. Dynamic PET imaging was performed over 30 minutes, with data reconstructed into 23 frames of different durations: 30 seconds, 6 × 5 seconds, 4 × 10 seconds, 6 × 30 seconds, 3 × 120 seconds, and 4 × 300 seconds.

2.3. Image processing methodology and statistical analysis

A comprehensive dynamic FDG-PET image analysis of the brain was performed using PMOD software (version 3.7, PMOD Technologies LLC, Zurich). To ensure anatomical precision and consistency across subjects, the analysis involved semi-automatic elastic registration to W. Schiffer's reference rat brain atlas (Schiffer et al., 2006), segmenting the brain into 58 distinct regions (see Supplementary Data 2 for the list of brain regions) (Fig. 1C). Temporal FDG uptake profiles within these 58 delineated brain regions were computed using a two-tissue compartment model to derive the time-activity curves (TACs) representing the mean FDG uptake kinetics in each region. To extract the arterial input function (AIF) (representing the radiotracer concentration in arterial blood for each animal), an image-derived input function (IDIF) was employed as a non-invasive alternative. For this purpose, a region of interest (ROI) was manually delineated in the *vena cava* on a dynamic PET frame acquired approximately 60 ± 5 seconds after FDG bolus injection (Lanz et al., 2014), a time point at which vascular activity was distinguishable, and the IDIF was derived from the *vena cava* time-activity using the model of Alf et al. (2013):

$$\frac{A_p}{A_b} = 0.51 \times e^{-0.1447 \times t(min)} + 0.3 \times e^{-0.00206 \times t(min)} + 0.8 \quad (1)$$

where A_p denotes plasma activity, and A_b denotes whole blood activity.

A two-tissue compartmental kinetic analysis based on the TACs and the derived IDIF yielded the kinetic constants reflecting glucose metabolism: K1 describing blood to tissue inflow, and k3 describing the phosphorylation of FDG by hexokinases (Fig. 1D). These two descriptors of FDG kinetics in 58 cerebral regions at three different time points (n = 5 animals per time point) yielded a comprehensive database of 1740 descriptors, i.e., 2 metabolic descriptors (K1 and k3) × 5 rats per time interval × 3-time intervals × 58 regions, which was used to analyze regional cerebral metabolic during disease progression. Metabolic changes between the acute and recovery phases were assessed on a cerebral region-wise basis against the pre-stress mean values using univariate Student's t-tests. Statistical significance was determined with a confidence level of 95 % (i.e., p-value ≤ 0.05). To quantify significance, we expressed the results as normalized z-scores, reflecting significant deviations from the pre-stress values normalized by the standard deviations.

2.4. Coordinated regional metabolic responses in brain areas

Interregional coordinated metabolic responses were assessed by computing statistical associations between regional metabolic parameters, following approaches adapted from Grosch et al. (2021) and Jamadar et al. (2021). Briefly, Pearson correlation coefficients (|r|) were calculated between all pairs of brain regions for each kinetic constant (K1 and k3) at baseline, acute, and recovery phases. Significant correlations ($|r| \geq 0.9, p \leq 0.05$) were interpreted as indicators of coordinated metabolic behavior. The resulting correlation matrices were structured as lower triangular matrices, excluding diagonal elements to avoid self-correlations. Brain regions were categorized into functional brain areas (parietal, retrosplenial, limbic, sensorimotor, audiovestibular, midbrain, and cerebellar), and the number of statistically significant correlations between brain regions belonging to each functional area was quantified (Fig. 1E).

3. Results

3.1. Cerebral FDG uptake during the acute phase of TTS

Fig. 2 shows z-score normalized deviations of FDG kinetic constants after ISO administration across brain regions, relative to their pre-stress values. During the acute phase of TTS (blue bars in Fig. 2), both K1 and

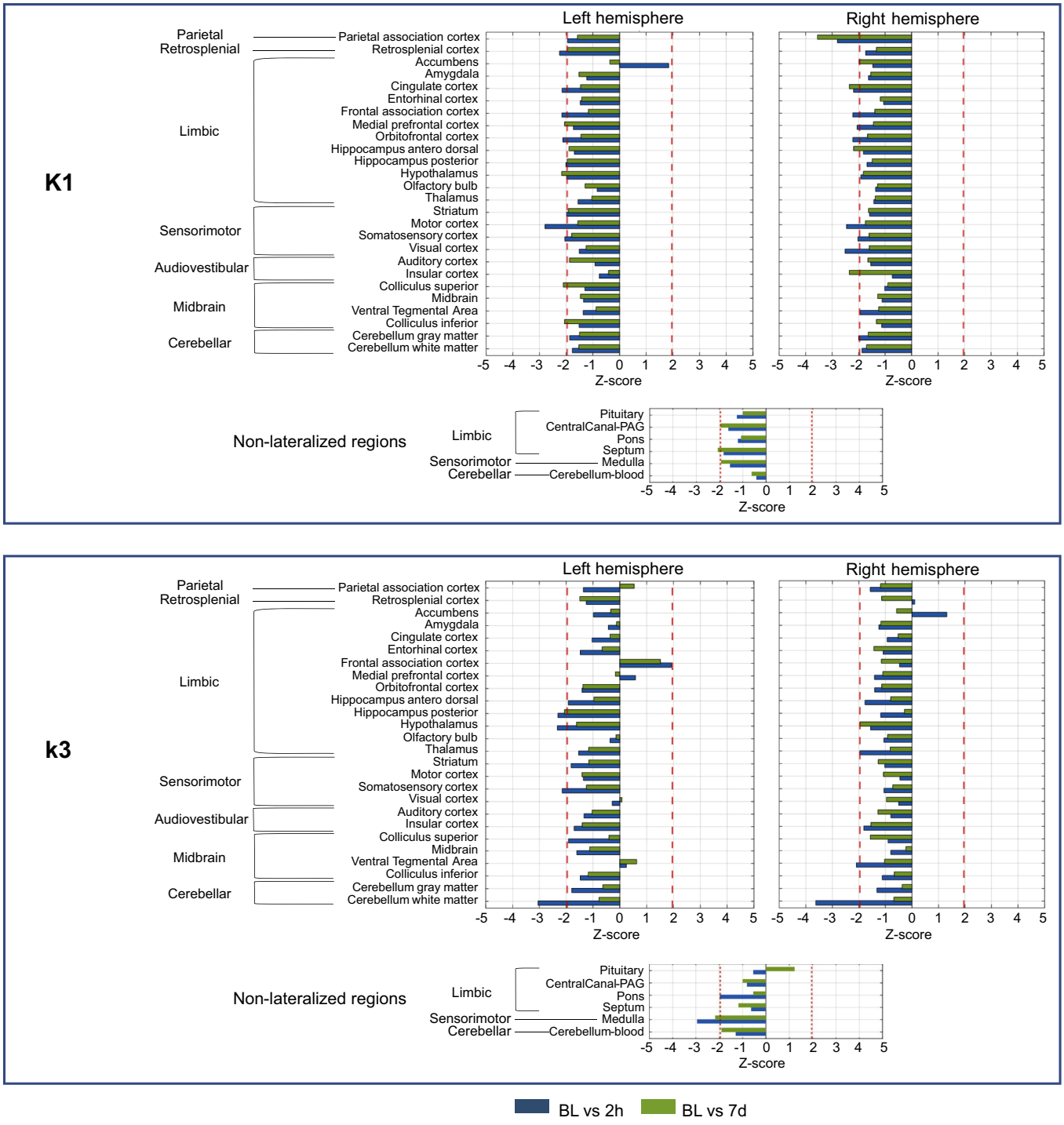

Fig. 2. Univariate analysis of metabolic constants K1 and k3 across brain regions during TTS progression. Relative changes in metabolic constants are expressed as normalized z-scores from t-tests (p-value ≤ 0.05), comparing pre-stress with the acute phase (2h) and pre-stress with the recovery phase (7d) ($n = 5$ rats per phase). Anatomical brain regions were grouped into separate functional areas for the right and left hemispheres and for non-lateralized regions. Blue bars: acute phase relative to pre-stress levels; green bars: recovery phase relative to pre-stress levels. Red dashed vertical lines denote significance thresholds (t-test).

k3 decreased broadly, with statistically significant reductions in 19 of 58 regions for K1 (33 %) and 9 regions for k3 (16 %). The largest K1 and k3 declines occurred in bilateral parietal and retrosplenial cortices and in structures of the limbic and sensorimotor areas. These findings indicate a widespread but region-specific metabolic depression, with glucose delivery from blood to tissue (i.e., K1) being more affected than phosphorylation (i.e., k3) during the acute catecholaminergic surge. Complete regional statistics are provided in Supplementary Data 3.

3.2. Cerebral FDG uptake during the recovery phase of TTS

During the recovery phase, one week after ISO challenge (green bars in Fig. 2), most brain regions maintained reduced K1 relative to their pre-stress values, as indicated by persistent negative z-scores. Although metabolic suppression remained widespread, attenuation of K1 reductions was observed in 60 % of regions, while 40 % showed further decreases, suggesting a heterogeneous recovery dynamic across brain

regions. Statistically significant reductions in K1 were identified in 11 regions (19 %).

Regarding k3 during the recovery phase, one week after ISO challenge, most regions showed reduced values relative to baseline. However, the overall magnitude of changes was smaller than during the acute phase, and statistically significant reductions in k3 were found only in 2 regions (3 %). Interestingly, the most significant changes for both K1 and k3 were predominantly localized in the limbic and sensorimotor areas, which are both composed of a large number of regions.

3.3. Coordinated regional metabolic responses in brain areas

We then examined the degree of coordination, defined as the number of significant interregional correlations between the metabolic responses within functional areas. The analysis focused on the regions with the largest absolute deviations of K1 and k3 relative to the pre-stress baseline, namely the limbic and sensorimotor regions (Fig. 3).

In the acute phase, the limbic area exhibited a substantial increase in coordinated K1 responses, with the number of significant correlations rising from 215 to 303 (+41 %), indicating enhanced synchronization of glucose inflow. In contrast, coordinated k3 responses markedly declined, from 294 to 149 (–49 %), reflecting disrupted coupling of glucose phosphorylation across limbic regions. The sensorimotor area showed a smaller increase in K1 correlations (from 32 to 34; +6 %) and a notable decrease in k3 correlations (from 35 to 15; –57 %).

During the recovery phase, the number of K1 correlations in the limbic area remained high (n=300, +40 % vs. baseline), suggesting persistent coordination of glucose inflow. However, k3 coordination

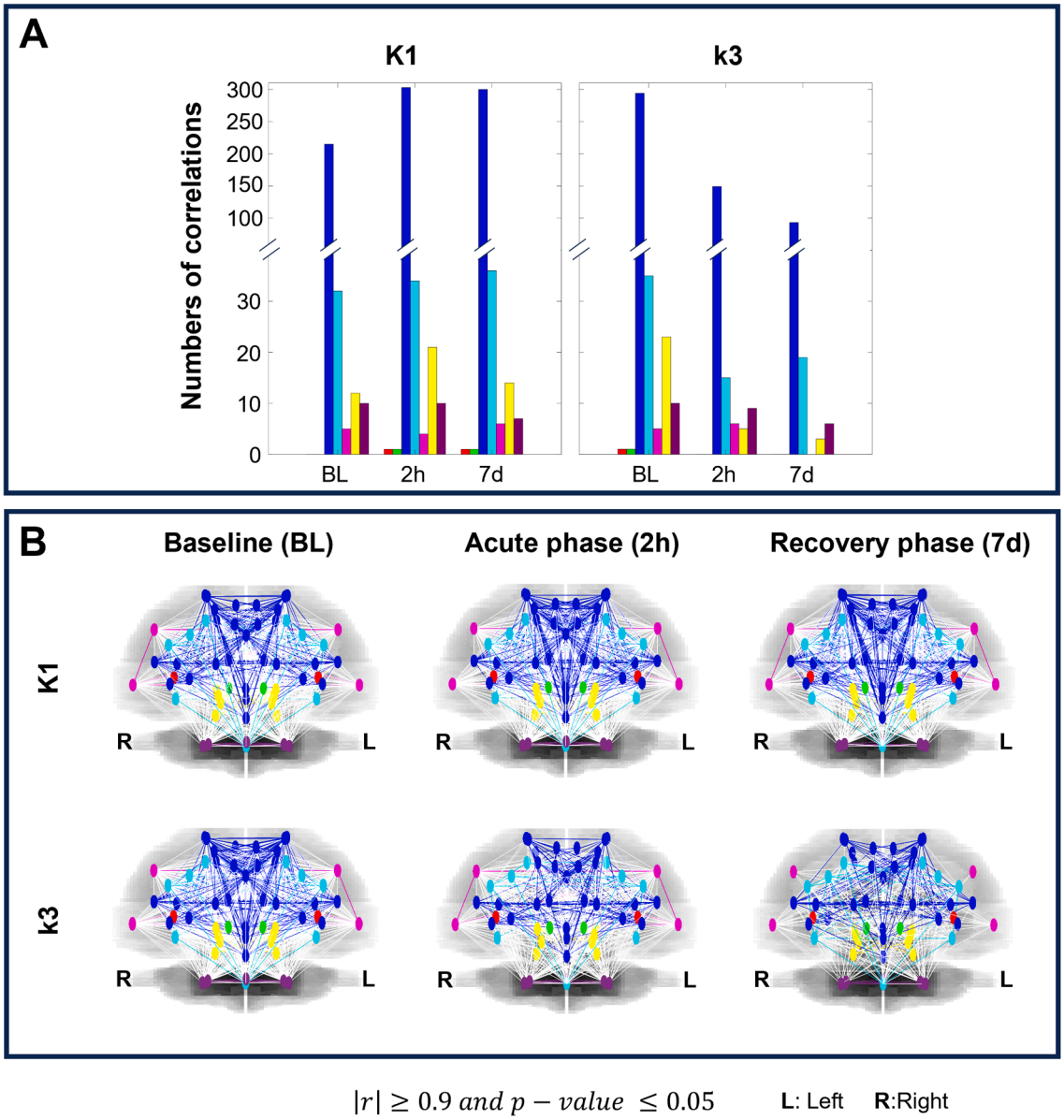

Fig. 3. Coordinated regional metabolic responses across stress phases, grouped by functional areas (BL: baseline; 2h: acute phase; 7d: recovery phase). A) Bar plot showing the number of statistically significant interregional correlations ($|r| \geq 0.9, p \leq 0.05$) between cerebral regions for the kinetic parameters K1 (glucose inflow) and k3 (glucose phosphorylation), calculated using Pearson's correlation analysis ($n = 5$ rats per phase). Correlations are grouped and color-coded by functional brain areas: parietal (red), retrosplenial (green), limbic (blue), sensorimotor (cyan), audiovestibular (magenta), midbrain (yellow), and cerebellar (purple). B) Spatial representation of these significant correlations, overlaid on a grey-scale horizontal projection of the W. Schiffer rat brain atlas (Schiffer et al., 2006). Colored lines are the coordinated metabolic responses within one functional area (colors are the same as in A). White lines indicate significant correlations between regions from different functional brain areas.

dropped sharply (n=93, –68 %), indicating a breakdown in the synchronization of phosphorylation processes. In the sensorimotor area, K1 correlations further increased slightly (n=36, +13 %), while k3 correlations remained reduced (from 35 to 19; –46 %).

Discussion

ISO administration is used in animal studies to induce a pharmacological stress that recapitulates the major cardiac signs of TTS (Godsman et al., 2022; Yoganathan et al., 2023; Zulfaj et al., 2024). In the present study, we show that, in addition to the changes in cardiac metabolism and function (Yoganathan et al., 2023), ISO induces significant alterations of cerebral glucose metabolism, both immediately (acute effect, 2 hours post-ISO) and after apparently complete recovery (recovery phase, 7 days post-ISO). Specifically, we observe widespread reductions of K1 constant during the acute phase, indicating decreased FDG transport from blood to brain in multiple regions. Though less pronounced, K1 reductions persist into the recovery phase, demonstrating that a single acute catecholaminergic stress has a sustained impact on brain glucose dynamics.

Glucose is the brain's primary energy substrate, supporting essential neuronal functions such as neurotransmitter synthesis and cellular homeostasis. Under physiological conditions, neuronal activity, cerebral blood flow (CBF), and glucose metabolism are tightly coupled, forming the basis of neurovascular and neurometabolic regulation (McKenna et al., 2012). FDG-PET kinetic modeling is a well-established technique to quantify cerebral glucose metabolism, yielding measurements of K1 and k3, the surrogate parameters for glucose cellular delivery and phosphorylation, respectively. Low K1 reflects decreased glucose delivery to brain tissue, which may result from altered transporter function, reduced vascular flow, or low metabolic demand. The persistence of altered K1 and k3 values into the recovery phase suggests that the catecholaminergic surge produces long-lasting disruptions in cerebral glucose metabolism after stress-induced signs have returned to normal. Since ISO is cleared from the blood in a few hours, changes in FDG kinetics seven days after its administration indicate delayed and long-lasting changes in brain metabolism. Although a transient impact on CBF or blood-brain barrier permeability during the acute phase cannot be entirely excluded, previous studies have provided limited evidence for significant or lasting changes in these parameters (Mitchell et al., 1975; Olesen et al., 1978; Murphy and Johanson, 1985; Olesen, 1986). Therefore, K1 and k3 changes reflect downstream effects on glucose transporter expression or intracellular glucose-processing pathways that persist well after the catecholamine levels have returned to normal values.

Acute phase reductions in both K1 and k3 were particularly prominent in brain regions involved in autonomic regulation and emotional processing: in the limbic and sensorimotor areas, associating the catecholamine-induced stress with hypometabolism shown by quantitative regional FDG-PET imaging. Sparse interhemispheric asymmetries were also observed in specific regions. The asymmetry observed in K1 in the acute phase, with a selective increase in the left nucleus accumbens, reflects an acute, lateralized neurovascular response. This is likely driven by the differential and asymmetric engagement of adrenergic receptors on the microvasculature, impacting CBF and glucose delivery in this limbic area following the peripheral catecholamine challenge (Raichle et al., 1975). In contrast, the asymmetry observed in k3 suggests a lateralized neurometabolic failure. The right cerebral hemisphere, particularly the prefrontal cortex, is known to exert dominant regulatory control over the sympathetic nervous system. The reduced k3 indicates a profound metabolic exhaustion or active functional suppression in this key top-down control circuit as it attempts to manage the overwhelming sympathetic stress (McKlveen et al., 2015). These persistent, sustained metabolic alterations, especially the asymmetric functional disruption in right-hemisphere circuits governing stress regulation, offer a plausible metabolic basis for the chronic cognitive and emotional disturbances reported in TTS patients. Moreover, the observation that patients with pre-existing neurological disorders experience worse long-term outcomes after TTS admission suggests that an acute, lateralized metabolic collapse in the frontal regulatory system could create a lasting vulnerability, contributing to increased long-term morbidity and mortality in this susceptible TTS population.

It is noteworthy that, in the preclinical TTS model used here, stress was induced by a peripheral pharmacological challenge, and not by a CNS-borne emotional stressor as in the so-called "broken heart syndrome". This is a clear indication that the regional metabolic alterations reported here are a consequence of cerebral dysfunction induced by the circulating catecholaminergic surge, and/or by its consequences outside the CNS. Even more surprising, during the recovery phase, a parallel decrease in both K1 and k3 was observed, particularly in the limbic area, which raises the question as to why there is a lack of compensatory mechanisms able to restore local metabolic balance in the CNS, possibly creating long-lasting altered neuronal activity and/or glial support after the initial catecholaminergic stress.

Metabolic correlation analysis revealed a significant divergence between K1 and k3 in the interregional metabolic associations throughout the progression of TTS. Regarding K1, the number of significant correlations between brain regions increased during both the acute and recovery phases relative to pre-stress, suggesting a global synchronization of glucose distribution. Concerning the acute phase, this is likely due to the systemic action of high ISO concentrations in the blood during stress, but there is no obvious explanation for its continuation, even dimmed at later times during recovery. In contrast, for k3 there was a sustained decrease in interregional correlations in both phases, indicating a breakdown of intracellular metabolic coordination of phosphorylation processes, suggesting heterogeneity of glucose metabolism across brain regions. These changes were most prominent in the limbic and sensorimotor areas, in line with their key functional role in the response to stress. Taken together, these findings reveal a pattern of prolonged stress-induced metabolic disruption that not only persists but is characterized by a globally decreased but more metabolically coordinated glucose inflow between regions, while phosphorylation capacity remains uncoordinated and globally decreased. Whether this pattern represents dysfunctional dynamic remodeling of the metabolic architecture of the brain and is linked to neuronal and/or glial metabolic dysfunction remains to be determined. It is interesting to parallel this observation with the fact that in cardiac tissue, using the same model, alternative pathways of glucose utilization are activated (Yoganathan et al., 2023).

Previous studies have shown functional (Silva et al., 2019; Templin et al., 2019; Dichtl et al., 2020; Khan et al., 2023) and metabolic (Radfar et al., 2021; Suzuki et al., 2021) alterations in brain regions involved in emotional processing and autonomic control in TTS patients. In retrospective analyses of FDG-PET scans, Tawakol and colleagues reported a greater risk of subsequent cardiovascular events (Tawakol et al., 2017) and TTS (Radfar et al., 2021) in patients who had high resting-state amygdala activity, suggesting that perceived stress was a cardiovascular risk factor, at least in cancer patients. In a *tour de force* follow-up study of 4 TTS patients imaged at 2-4 days ("acute" phase) and 29-40 days (recovery phase), Suzuki et al. (2021) performed similar FDG-PET imaging and showed a reversible increase of amygdala activation.

Our results are in line with fMRI studies in TTS patients (Silva et al., 2019; Templin et al., 2019; Khan et al., 2023) showing reduced activity (Templin et al., 2019), connectivity (Silva et al., 2019), and anatomical anomalies (Khan et al., 2023) in TTS patients, mostly in cerebral areas covering the limbic system and the autonomic nervous system. They are also in apparent contradiction with brain FDG-PET studies in TTS patients that reported increased amygdala activity (Radfar et al., 2021; Suzuki et al., 2021), while we show sustained glucose hypometabolism in our TTS animal model. Several reasons may explain this discrepancy. Firstly, the TTS-inducing trigger is different in our model (peripheral

administration of catecholamine) and in patients (mental stress centrally originating in the CNS). Secondly, the animal model yielded direct measurements of cerebral kinetic constants K1 and k3, reflecting cerebral uptake and phosphorylation of glucose, while the clinical measurements were based on ratios of amygdala to total brain uptake of FDG at a fixed time point, one hour post FDG injection, as reported by Radfar et al. (2021), not mentioned in Suzuki et al. (2021). Thirdly, several small studies have shown a discrepancy called "inverse flow mismatch" in TTS patients between metabolism assessed by FDG-PET and flow assessed by nuclear imaging of myocardial perfusion (Bybee et al., 2006), reviewed in Testa and Feola (2014). It would be interesting to use MRI-PET techniques to test whether this is also the case in TTS patients or animal models.

Further research on TTS is needed to define the potential benefit of measuring cerebral glucose metabolic constants in TTS. This may be useful to address the molecular mechanisms underlying persistent metabolic alterations, therefore possibly predicting the risk of long-term neuropsychiatric sequelae in TTS patients. Eventually, it could lead to the identification of novel therapeutic targets aimed at preserving brain function and improving long-term outcomes in vulnerable populations.

We confirm here our previous results obtained in cardiac FDG-PET studies in the same animal models (Yoganathan et al., 2023), showing that an acute catecholamine surge triggers a cascade of events leading to long-term changes in glucose handling by tissues, including the CNS. Several mechanisms can be called upon to explain the action of peripheral catecholamine on cerebral metabolism. Firstly, the cardiac dysfunction characterized by basal hypercontractility and apical akinesia may contribute to the impairment of cerebral metabolism, acute myocardial dysfunction leading to systemic metabolic dysregulation affecting both the heart and brain. Secondly, systematically altered glucose handling could influence cerebral metabolism through neurohumoral mechanisms or altered autonomic regulation. Thirdly, the involvement of specific brain regions, particularly within the limbic system, may also be related to the regional distribution of adrenergic receptors. It has been shown that the apex of the LV, the cardiac region in which akinesia is most frequently observed during TTS, has a higher density and sensitivity of β-adrenergic receptors (Lyon et al., 2008). The limbic system includes the amygdala, hippocampus, and insula, and is known to play major roles in emotional processing and autonomic nervous system control. It is therefore tempting to suggest that dysfunctional cerebral metabolic remodeling may reflect hypoactivation or a low compensatory response in these regions. Indeed, clinical studies have reported a high frequency of pre-existing neurological disorders in TTS patients, which have increased short- and long-term mortality rates relative to patients without such condition (Herman et al., 2016; Cammann et al., 2021; Suzuki et al., 2021; Leissner et al., 2025). Persistent hypometabolism and disrupted metabolic coordination, particularly within the limbic system, may provide a metabolic basis for the cognitive and emotional disturbances frequently observed in TTS patients.

Study limitations. The use of an animal model to mimic human TTS has several limitations. Firstly, the induction of TTS by the administration of catecholamine is only one of the several types of triggers inducing TTS in patients, and it does not encompass the broader spectrum of triggering factors (mental or physical stress, neurological or systemic events). Here, the catecholaminergic surge, the common mechanism of TTS, whatever its triggering factor, has a peripheral origin in contrast to acute mental stress originating from the CNS or even peripheral physical stress, e.g., surgery, stroke, bleeding, giving birth, among others. Moreover, the model omits common comorbidities of mid- to late-life patients (e.g., hypertension, diabetes, obesity) and uses young adult female rats, whereas clinical TTS is most prevalent in post-menopausal women. Secondly, in animals, FDG-PET imaging was performed under anesthesia, which may modulate FDG uptake and thereby influence the cerebral response to a catecholaminergic challenge. However, by mitigating this effect through continuous physiological monitoring and carefully titrating anesthetic depth and temperature to maintain stable, comparable conditions across groups, we are confident that the observed differences in FDG uptake represent genuine biological changes induced by acute stress rather than confounding effects of anesthesia. Thirdly, cerebral connectivity is lower in rodents than in humans, and, finally, it cannot be excluded that regional connectivity differs between the two species. However, fMRI studies agree with our results and suggest that metabolic changes are an important aspect of TTS.

The translation of our results in an animal model to the clinical situation deserves caution, considering the multifactorial etiology of TTS. Our experiments deliberately target a single critical mechanism, the acute catecholaminergic surge and its metabolic sequelae in regional cerebral metabolism. Further studies in human patients are needed to confirm our preclinical results.

4. Conclusion

In summary, anomalies of cerebral glucose utilization are a central and persistent feature of the response to acute catecholaminergic stress in the rat model of TTS. Cerebral hypometabolism and disrupted interregional coordination of metabolic activity occur early and persist beyond behavioral signs of recovery, suggesting that the brain remains metabolically altered long after the peripheral symptoms have subsided. These findings support the importance of including cerebral metabolic measures in experimental models of stress cardiomyopathy and underscore the potential role of bidirectional brain-heart interactions in TTS pathophysiology. They also advocate for a holistic approach to TTS to recognize its potential to compromise both cardiac and cerebral functions. Integrated care strategies that explicitly address the interplay between the heart and brain may be crucial for optimizing long-term recovery and well-being in TTS patients (Hovgaard et al., 2019).

Data and code availability statement

Data are obtainable from the corresponding author upon reasonable request.

CRediT authorship contribution statement

Alejandro Ariza-Carrasco: Writing – review & editing, Writing – original draft, Visualization, Validation, Software, Methodology, Investigation, Formal analysis, Data curation, Conceptualization. **Thulaciga Yoganathan:** Writing – review & editing, Writing – original draft, Visualization, Validation, Software, Methodology, Investigation, Formal analysis, Data curation, Conceptualization. **María Alonso de Leciñana:** Writing – review & editing, Conceptualization. **Thomas Viel:** Writing – review & editing. **Nidaa Mikail:** Writing – review & editing, Writing – original draft, Conceptualization. **Joaquin L. Herraiz:** Writing – review & editing, Writing – original draft, Conceptualization. **Jose M. Udias:** Writing – review & editing, Writing – original draft, Conceptualization. **Paula Ibáñez:** Writing – review & editing, Funding acquisition, Conceptualization. **Bertrand Tavitian:** Writing – review & editing, Writing – original draft, Supervision, Resources, Project administration, Investigation, Funding acquisition, Formal analysis, Conceptualization. **Mailyn Pérez-Liva:** Writing – review & editing, Writing – original draft, Validation, Supervision, Resources, Project administration, Methodology, Investigation, Funding acquisition, Formal analysis, Conceptualization.

Declaration of competing interest

The authors declare that they have no known competing financial interests or personal relationships that could have appeared to influence the work reported in this paper.

Acknowledgements

MP-L acknowledges support from the Programme Ramón y Cajal RYC2021-032739-I, funded by MCIN/AEI/10.13039/501100011033 and by the European Union "NextGenerationEU"/PRTR". JLH acknowledges support from grants FASCINA (PID2021-126998OB-I00/), 3PET (PDC2022-133057-I00), Prototwin Project (TED2021-130592B-I00) from the Spanish Ministry of Science and Innovation (MCIN) AEI/10.13039/501100011033/Unión Europea Next GenerationEU/PRTR, and "Tecnologías Avanzadas para la Exploración del Universo y sus Componentes" (PR47/21 TAU-CM TAU-PRTR), funded by EU Resilient and NextGeneration funds. This work has been funded with €1.026 million by the Comunidad de Madrid through the LUNABRAIN-CM R&D activities program (TEC-2024/TEC-43), granted by Order 5696/2024, and has also received funding from the Cancer Research for Personalized Medicine – CARPEM project (Site de Recherche Intégré sur le Cancer SIRIC), from the Plan Cancer Physicancer [grant number C16025KS], and from the Région Ile-de-France SESAME funds. This work was supported by Knowledge Generation Projects 2022 Type A Oriented Research, Government of Spain PID2022-137114OA-I00. In vivo imaging was performed at the Life Imaging Facility of Université Paris Cité (Plateforme Imageries du Vivant - PIV), supported by France Life Imaging [grant number ANR-11-INBS-0006] and Infrastructures Biologie-Santé (IBiSa). BT, MP-L, PIG, JLH and JMU acknowledge support from the European Union as part of the European Innovation Council's Pathfinder Open Programme: RETIMAGER, 101099096.

Supplementary materials

Supplementary material associated with this article can be found, in the online version, at doi:10.1016/j.neuroimage.2026.121797.

References

Alf, M.F., Martić-Kehl, M.I., Schibli, R., Krämer, S.D., 2013. FDG kinetic modeling in small rodent brain PET: optimization of data acquisition and analysis. EJNMMI Res 3, 1–14. https://doi.org/10.1186/2191-219X-3-61.

Arri, S.S., Ryan, M., Redwood, S.R., Marber, M.S., 2016. Mental stress-induced myocardial ischaemia. Heart 102, 472–480. https://doi.org/10.1136/heartjnl-2014-307306.

Bybee, K.A., Murphy, J., Prasad, A., Wright, R.S., Lerman, A., Rihal, C.S., Chareonthaitawee, P., 2006. Acute impairment of regional myocardial glucose uptake in the apical ballooning (takotsubo) syndrome. J. Nucl. Cardiol. 13, 244–250. https://doi.org/10.1007/BF02971249.

Cammann, V.L., Scheitz, J.F., von Rennenberg, R., Jäncke, L., Nolte, C.H., Szawan, K.A., Stengl, H., Würdinger, M., Endres, M., Templin, C., Ghadri, J.R., 2021. Clinical correlates and prognostic impact of neurologic disorders in Takotsubo syndrome. Sci. Rep. 11, 23555. https://doi.org/10.1038/s41598-021-01496-9.

Cannon, W.B., 1915. Bodily changes in pain, hunger, fear, and rage. D. Appleton and Company, New York.

Carey, I.M., Shah, S.M., DeWilde, S., Harris, T., Victor, C.R., Cook, D.G., 2014. Increased risk of acute cardiovascular events after partner bereavement: a matched cohort study. JAMA Intern. Med. 174, 598–605. https://doi.org/10.1001/jamainternmed.2013.14558.

Collen, J., Bimson, W., Devine, P., 2008. A variant of Takotsubo cardiomyopathy: a rare complication in the electrophysiology lab. J. Invasive Cardiol. 20, E310–E313.

Dichtl, W., Tuovinen, N., Barbieri, F., Adukauskaite, A., Senoner, T., Rubatscher, A., Hintringer, F., Siedentopf, C., Bauer, A., Gizewski, E.R., Steiger, R., 2020. Functional neuroimaging in the acute phase of takotsubo syndrome: volumetric and functional changes of the right insular cortex. Clin. Res. Cardiol. 109, 1107–1113. https://doi.org/10.1007/s00392-020-01602-3.

Dienel, G.A., 2019. Brain glucose metabolism: integration of energetics with function. Physiol. Rev. 99, 949–1045. https://doi.org/10.1152/physrev.00062.2017.

Dragano, N., Siegrist, J., Nyberg, S.T., Lunau, T., Fransson, E.I., Alfredsson, L., Bjorner, J. B., Borritz, M., Burr, H., Erbel, R., Fahlén, G., Goldberg, M., Hamer, M., Heikkilä, K., Jöckel, K.H., Knutsson, A., Madsen, I.E.H., Nielsen, M.L., Nordin, M., Oksanen, T., Pejtersen, J.H., Pentti, J., Rugulies, R., Salo, P., Schupp, J., Singh-Manoux, A., Steptoe, A., Theorell, T., Vahtera, J., Westerholm, P.J.M., Westerlund, H., Virtanen, M., Zins, M., Batty, G.D., Kivimäki, M., 2017. Effort–reward imbalance at work and incident coronary heart disease: a multicohort study of 90,164 individuals. Epidemiology 28, 619–626. https://doi.org/10.1097/EDE.0000000000000666.

Fernández-Cordón, C., Núñez-Gil, I.J., Martín de Miguel, I., Pérez-Castellanos, A., Vedia, O., Almendro-Delia, M., López-País, J., Uribarri, A., Duran-Cambra, A., Martín-García, A., Raposeiras-Roubin, S., Blanco-Ponce, E., Corbí-Pascual, M., Guillén Marzo, M., Andrés, M., Feltes, G., Martínez-Selles, M., 2023. Takotsubo syndrome, stressful triggers, and risk of recurrence. Am. J. Cardiol. 205, 58–62. https://doi.org/10.1016/j.amjcard.2023.07.155.

Ghadri, J.R., Kato, K., Cammann, V.L., Gili, S., Jurisic, S., Di Vece, D., Candreva, A., Ding, K.J., Micek, J., Szawan, K.A., Bacchi, B., Bianchi, R., Levinson, R.A., Wischnewsky, M., Seifert, B., Schlossbauer, S.A., Citro, R., Bossone, E., Münzel, T., Knorr, M., Heiner, S., D'Ascenzo, F., Franke, J., Sarcon, A., Napp, L.C., Jaguszewski, M., Noutsias, M., Katus, H.A., Burgdorf, C., Schunkert, H., Thiele, H., Bauersachs, J., Tschöpe, C., Pieske, B.M., Rajan, L., Michels, G., Pfister, R., Cuneo, A., Jacobshagen, C., Hasenfuß, G., Karakas, M., Koenig, W., Rottbauer, W., Said, S.M., Braun-Dullaeus, R.C., Banning, A., Cuculi, F., Kobza, R., Fischer, T.A., Vasankari, T., Airaksinen, K.E.J., Opolski, G., Dworakowski, R., MacCarthy, P., Kaiser, C., Osswald, S., Galiuto, L., Crea, F., Dichtl, W., Empen, K., Felix, S.B., Delmas, C., Lairez, O., El-Battrawy, I., Akin, I., Borggrefe, M., Horowitz, J., Kozel, M., Tousek, P., Widimský, P., Gilyarova, E., Shilova, A., Gilyarov, M., Winchester, D.E., Ukena, C., Bax, J.J., Prasad, A., Böhm, M., Lüscher, T.F., Ruschitzka, F., Templin, C., 2018. Long-term prognosis of patients with takotsubo syndrome. J. Am. Coll. Cardiol. 72, 874–882. https://doi.org/10.1016/j.jacc.2018.06.016.

Gianni, M., Dentali, F., Grandi, A.M., Sumner, G., Hiralal, R., Lonn, E., 2006. Apical ballooning syndrome or takotsubo cardiomyopathy: a systematic review. Eur. Heart J. 27, 1523–1529. https://doi.org/10.1093/eurheartj/ehl032.

Godsman, N., Kohlhaas, M., Nickel, A., Cheyne, L., Mingarelli, M., Schweiger, L., Hepburn, C., Munts, C., Welch, A., Delibegovic, M., Van Bilsen, M., Maack, C., Dawson, D., 2022. Metabolic alterations in a rat model of takotsubo syndrome. Cardiovasc. Res. 118, 1932–1946. https://doi.org/10.1093/cvr/cvab081.

Grosch, M., Lindner, M., Bartenstein, P., Brandt, T., Dieterich, M., Ziegler, S., Zwergal, A., 2021. Dynamic whole-brain metabolic connectivity during vestibular compensation in the rat. Neuroimage 226, 117588. https://doi.org/10.1016/j.neuroimage.2020.117588.

Hayashi, T., Tiwary, S.K., Lim, K.R.Q., Rocha-Resende, C., Kovacs, A., Weinheimer, C., Mann, D.L., 2023. Refining the reproducibility of a murine model of stress-induced reversible cardiomyopathy. Am. J. Physiol. Heart Circ. Physiol. 324, H229–H240. https://doi.org/10.1152/ajpheart.00684.2022.

Heberden, W., 1802. Commentaries on the History and Cure of Diseases. T. Payne, London.

Herman, J.P., McKlveen, J.M., Ghosal, S., Kopp, B., Wulsin, A., Makinson, R., Scheimann, J., Myers, B., 2016. Regulation of the hypothalamic-pituitary-adrenocortical stress response. Compr. Physiol. 6, 603–664. https://doi.org/10.1002/cphy.c150015.

Hovgaard, H.L., Zaremba, T., Aaroe, J., 2019. Relapsing classical takotsubo syndrome in a postmenopausal woman successfully managed with psychology consultations. Cureus 11, e5361. https://doi.org/10.7759/cureus.5361.

Jamadar, S.D., Ward, P.G.D., Liang, E.X., Orchard, E.R., Chen, Z., Egan, G.F., 2021. Metabolic and hemodynamic resting-state connectivity of the human brain: a high-temporal resolution simultaneous BOLD-fMRI and FDG-fPET multimodality study. Cereb. Cortex 31, 2855–2867. https://doi.org/10.1093/cercor/bhaa393.

Khan, H., Gamble, D.T., Rudd, A., Mezincescu, A.M., Abbas, H., Noman, A., Stewart, A., Horgan, G., Krishnadas, R., Williams, C., Waiter, G.D., Dawson, D.K., 2023. Structural and functional brain changes in acute takotsubo syndrome. JACC Heart Fail 11, 307–317. https://doi.org/10.1016/j.jchf.2022.11.001.

Kivimäki, M., Kawachi, I., 2015. Work stress as a risk factor for cardiovascular disease. Curr. Cardiol. Rep. 17, 1–9. https://doi.org/10.1007/s11886-015-0630-8.

Kivimäki, M., Nyberg, S.T., Batty, G.D., Kawachi, I., Jokela, M., Alfredsson, L., Bjorner, J. B., Borritz, M., Burr, H., Dragano, N., Fransson, E.I., Heikkilä, K., Knutsson, A., Koskenvuo, M., Kumari, M., Madsen, I.E.H., Nielsen, M.L., Nordin, M., Oksanen, T., Pejtersen, J.H., Pentti, J., Rugulies, R., Salo, P., Shipley, M.J., Suominen, S., Theorell, T., Vahtera, J., Westerholm, P., Westerlund, H., Steptoe, A., Singh-Manoux, A., Hamer, M., Ferrie, J.E., Virtanen, M., Tabak, A.G., 2017. Long working hours as a risk factor for atrial fibrillation: a multi-cohort study. Eur. Heart J. 38, 2621–2628. https://doi.org/10.1093/eurheartj/ehx324.

Kivimäki, M., Steptoe, A., 2018. Effects of stress on the development and progression of cardiovascular disease. Nat. Rev. Cardiol. 15, 215–229. https://doi.org/10.1038/nrcardio.2017.189.

Laghlam, D., Touboul, O., Herry, M., Estagnasié, P., Dib, J.C., Baccouche, M., Brusset, A., Nguyen, L.S., Squara, P., 2023. Takotsubo cardiomyopathy after cardiac surgery: a case-series and systematic review of literature. Front. Cardiovasc. Med. 9, 1067444. https://doi.org/10.3389/fcvm.2022.1067444.

Lanz, B., Poitry-Yamate, C., Gruetter, R., 2014. Image-derived input function from the vena cava for 18F-FDG PET studies in rats and mice. J. Nucl. Med. 55, 1380–1388. https://doi.org/10.2967/jnumed.113.127381.

Leissner, P., Olsson, E.M.G., Rondung, E., Sundelin, R., Spaak, J., Ulvenstam, A., Nordenskjöld, A., Kövamees, L., Lyngå, P., Held, C., Tornvall, P., Humphries, S., 2025. Mental health status and quality-of-life after an acute myocardial infarction with non-obstructive coronary arteries or takotsubo syndrome: a systematic review. Eur. J. Prev. Cardiol., zwaf101 https://doi.org/10.1093/eurjpc/zwaf101.

Looi, J-L., Verryt, T., McLeod, P., Chan, C., Pemberton, J., Webster, M., To, A., Lee, M., Kerr, A.J., 2022. Type of stressor and medium-term outcomes after takotsubo syndrome: what becomes of the broken-hearted? (ANZACS-QI 59). Heart Lung Circ 31, 499–507. https://doi.org/10.1016/j.hlc.2021.09.021.

Lyon, A.R., Rees, P.S., Prasad, S., Poole-Wilson, P.A., Harding, S.E., 2008. Stress (Takotsubo) cardiomyopathy — A novel pathophysiological hypothesis to explain catecholamine-induced acute myocardial stunning. Nat. Rev. Cardiol. 5, 22–29. https://doi.org/10.1038/ncpcardio1066.

Madias, J.E., 2024. Left ventricular outflow tract obstruction/hypertrophic cardiomyopathy/takotsubo syndrome: a new hypothesis of takotsubo syndrome

pathophysiology. Curr. Probl. Cardiol. 49, 102668. https://doi.org/10.1016/j.cpcardiol.2024.102668.
Madias, J.E., 2025. Is takotsubo syndrome probably an acute coronary syndrome after all? Clin. Res. Cardiol. 114, 1–2. https://doi.org/10.1007/s00392-025-02646-z.
McKenna, M.C., Dienel, G.A., Sonnewald, U., Waagepetersen, H.S., Schousboe, A., 2012. Energy metabolism of the brain. In: Brady, S.T., Siegel, G.J., Albers, R.W. (Eds.), Basic Neurochemistry, eighth ed. Academic Press, Amsterdam, pp. 200–231. https://doi.org/10.1016/B978-0-12-374947-5.00011-0.
McKlveen, J.M., Myers, B., Herman, J.P., 2015. The medial prefrontal cortex: coordinator of autonomic, neuroendocrine and behavioural responses to stress. J. Neuroendocrinol. 27, 446–456. https://doi.org/10.1111/jne.12272.
Mitchell, G., Scriven, D.R., Rosendorff, C., 1975. Adrenoceptors in intracerebral resistance vessels. Br. J. Pharmacol. 54, 11–15. https://doi.org/10.1111/j.1476-5381.1975.tb07403.x.
Murphy, V.A., Johanson, C.E., 1985. Adrenergic-induced enhancement of brain barrier system permeability to small nonelectrolytes: choroid plexus versus cerebral capillaries. J. Cereb. Blood Flow Metab. 5, 401–412. https://doi.org/10.1038/jcbfm.1985.55.
Nyman, E., Mattsson, E., Tornvall, P., 2019. Trigger factors in takotsubo syndrome – a systematic review of case reports. Eur. J. Intern. Med. 63, 62–68. https://doi.org/10.1016/j.ejim.2019.02.017.
Olesen, J., Hougård, K., Hertz, M., 1978. Isoproterenol and propranolol: ability to cross the blood-brain barrier and effects on cerebral circulation in man. Stroke 9, 344–353. https://doi.org/10.1161/01.STR.9.4.34.
Olesen, J., 1986. Beta-adrenergic effects on cerebral circulation. Cephalalgia 6, 41–46. https://doi.org/10.1177/03331024860060S505.
Pelliccia, F., Pasceri, V., Patti, G., Tanzilli, G., Speciale, G., Gaudio, C., Camici, P.G., 2019. Long-term prognosis and outcome predictors in takotsubo syndrome: a systematic review and meta-regression study. J. Am. Coll. Cardiol. HF. 7, 143–154. https://doi.org/10.1016/j.jchf.2018.10.009.
Radfar, A., Abohashem, S., Osborne, M.T., Wang, Y., Dar, T., Hassan, M.Z., Ghoneem, A., Naddaf, N., Patrich, T., Abbasi, T., Zureigat, H., Jaffer, J., Ghazi, P., Scott, J.A., Shin, L.M., Pitman, R.K., Neilan, T.G., Wood, M.J., Tawakol, A., 2021. Stress-associated neurobiological activity associates with the risk for and timing of subsequent takotsubo syndrome. Eur. Heart J. 42, 1898–1908. https://doi.org/10.1093/eurheartj/ehab029.
Raichle, M.E., Hartman, B.K., Eichling, J.O., Sharpe, L.G., 1975. Central noradrenergic regulation of cerebral blood flow and vascular permeability. Proc. Natl. Acad. Sci. 72, 3726–3730. https://doi.org/10.1073/pnas.72.9.3726.
Redfors, B., Ali, A., Shao, Y., Lundgren, J., Gan, L.M., Omerovic, E., 2014. Different catecholamines induce different patterns of takotsubo-like cardiac dysfunction in an apparently afterload-dependent manner. Int. J. Cardiol. 174, 330–336. https://doi.org/10.1016/j.ijcard.2014.04.103.
Santoro, F., Núñez Gil, I.J., Stiermaier, T., El-Battrawy, I., Guerra, F., Novo, G., Guastafierro, F., Tarantino, N., Novo, S., Mariano, E., Romeo, F., Capucci, A., Bahlmann, E., Zingaro, M., Cannone, M., Caldarola, P., Marchetti, M.F., Montisci, R., Meloni, L., Thiele, H., Di Biase, M., Almendro-Delia, M., Sionis, A., Akin, I., Eitel, I., Brunetti, N.D., 2019. Assessment of the German and Italian stress cardiomyopathy score for risk stratification for in-hospital complications in patients with takotsubo syndrome. JAMA Cardiol. 4, 892–899. https://doi.org/10.1001/jamacardio.2019.2597.
Santoro, F., Núñez Gil, I.J., Arcari, L., Vitale, E., Martino, T., El-Battrawy, I., Guerra, F., Novo, G., Mariano, E., Musumeci, B., Cacciotti, L., Caldarola, P., Montisci, R., Ragnatela, I., Cetera, R., Vedia, O., Blanco, E., Lopez Pais, J., Martin, A., Pérez-Castellanos, A., Salamanca, J., Bartolomucci, F., Akin, I., Thiele, H., Eitel, I., Stiermaier, T., Brunetti, N.D., 2024. Neurological disorders in takotsubo syndrome: clinical phenotypes and outcomes. J. Am. Heart Assoc. 13, e032128. https://doi.org/10.1161/JAHA.123.032128.
Sarmiento, L.F., Ríos-Flórez, J.A., Rincón Uribe, F.A., Rodrigues Lima, R., Kalenscher, T., Gouveia Jr, A., Nitsch, F.J., 2024. Do stress hormones influence choice? A systematic review of pharmacological interventions on the HPA axis and/or SAM system. Soc. Cogn. Affect. Neurosci. 19, nsae069. https://doi.org/10.1093/scan/nsae069.
Satyavolu, B., Neupane, G., Topacio, T., Patel, P., Freher, M., 2022. A case of isoproterenol-induced takotsubo syndrome. J. Am. Coll. Cardiol. 79 (Suppl 9), 2690. https://doi.org/10.1016/S0735-1097(22)03681-6.
Scally, C., Rudd, A., Mezincescu, A., Wilson, H., Srivanasan, J., Horgan, G., Broadhurst, P., Newby, D.E., Henning, A., Dawson, D.K., 2018. Persistent long-term structural, functional, and metabolic changes after stress-induced (Takotsubo) cardiomyopathy. Circulation 137, 1039–1048. https://doi.org/10.1161/CIRCULATIONAHA.117.031841.
Schiffer, W.K., Mirrione, M.M., Biegon, A., Alexoff, D.L., Patel, V., Dewey, S.L., 2006. Serial microPET measures of the metabolic reaction to a microdialysis probe implant. J. Neurosci. Methods 155, 272–284. https://doi.org/10.1016/j.jneumeth.2006.01.027.
Selye, H., 1950. Stress: the physiology and pathology of exposure to stress. Acta Medica Publication, Montreal.
Shams, Y., 2016. Clinical features and outcome of pheochromocytoma-induced takotsubo syndrome: analysis of 80 published cases. Am. J. Cardiol. 117, 1836–1844. https://doi.org/10.1016/j.amjcard.2016.03.019.
Silva, A.R., Magalhães, R., Arantes, C., Moreira, P.S., Rodrigues, M., Marques, P., Marques, J., Sousa, N., Pereira, V.H., 2019. Brain functional connectivity is altered in patients with takotsubo syndrome. Sci. Rep. 9, 4187. https://doi.org/10.1038/s41598-019-40695-3.
Singh, T., Khan, H., Gamble, D.T., Scally, C., Newby, D.E., Dawson, D., 2022. Takotsubo syndrome: pathophysiology, emerging concepts, and clinical implications. Circulation 145, 1002–1019. https://doi.org/10.1161/CIRCULATIONAHA.121.055854.
Stiermaier, T., Moeller, C., Oehler, K., Desch, S., Graf, T., Eitel, C., Vonthein, R., Schuler, G., Thiele, H., Eitel, I., 2016. Long-term excess mortality in takotsubo cardiomyopathy: predictors, causes and clinical consequences. Eur. J. Heart Fail. 18, 650–656. https://doi.org/10.1002/ejhf.494.
Suzuki, H., Takanami, K., Takase, K., Shimokawa, H., Yasuda, S., 2021. Reversible increase in stress-associated neurobiological activity in the acute phase of takotsubo syndrome: a brain 18F-FDG-PET study. Int. J. Cardiol. 344, 31–33. https://doi.org/10.1016/j.ijcard.2021.09.057.
Tawakol, A., Ishai, A., Takx, R.A.P., Figueroa, A.L., Ali, A., Kaiser, Y., Truong, Q.A., Solomon, C.J.E., Calcagno, C., Mani, V., Tang, C.Y., Mulder, W.J.M., Murrough, J. W., Hoffmann, U., Nahrendorf, M., Shin, L.M., Fayad, Z.A., Pitman, R.K., 2017. Relation between resting amygdalar activity and cardiovascular events: a longitudinal and cohort study. Lancet 389, 834–845. https://doi.org/10.1016/S0140-6736(16)31714-7.
Templin, C., Ghadri, J.R., Diekmann, J., Napp, L.C., Bataiosu, D.R., Jaguszewski, M., Cammann, V.L., Sarcon, A., Geyer, V., Neumann, C.A., Seifert, B., Hellermann, J., Schwyzer, M., Eisenhardt, K., Jenewein, J., Franke, J., Katus, H.A., Burgdorf, C., Schunkert, H., Moeller, C., Thiele, H., Bauersachs, J., Tschöpe, C., Schultheiss, H-P., Laney, C.A., Rajan, L., Michels, G., Pfister, R., Ukena, C., Böhm, M., Erbel, R., Cuneo, A., Kuck, K-H., Jacobshagen, C., Hasenfuss, G., Karakas, M., Koenig, W., Rottbauer, W., Said, S.M., Braun-Dullaeus, R.C., Cuculi, F., Banning, A., Fischer, T. A., Vasankari, T., Airaksinen, K.E.J., Fijalkowski, M., Rynkiewicz, A., Pawlak, M., Opolski, G., Dworakowski, R., MacCarthy, P., Kaiser, C., Osswald, S., Galiuto, L., Crea, F., Dichtl, W., Franz, W.M., Empen, K., Felix, S.B., Delmas, C., Lairez, O., Erne, P., Bax, J.J., Ford, I., Ruschitzka, F., Prasad, A., Lüscher, T.F., 2015. Clinical features and outcomes of takotsubo (stress) cardiomyopathy. N. Engl. J. Med. 373, 929–938. https://doi.org/10.1056/NEJMoa1406761.
Templin, C., Hänggi, J., Klein, C., Topka, M.S., Hiestand, T., Levinson, R.A., Jurisic, S., Lüscher, T.F., Ghadri, J.R., Jäncke, L., 2019. Altered limbic and autonomic processing supports brain-heart axis in takotsubo syndrome. Eur. Heart J. 40, 1183–1187. https://doi.org/10.1093/eurheartj/ehz068.
Testa, M., Feola, M., 2014. Usefulness of myocardial positron emission tomography/nuclear imaging in takotsubo cardiomyopathy. World J. Radiol. 6, 502–506. https://doi.org/10.4329/wjr.v6.i7.502.
Wang, X., Pei, J., Hu, X., 2020. The brain-heart connection in takotsubo syndrome: the central nervous system, sympathetic nervous system, and catecholamine overload. Cardiol. Res. Pract. 2020, 4150291. https://doi.org/10.1155/2020/4150291.
Wang, T., Xiong, T., Yang, Y., Zuo, B., Chen, X., Wang, D., 2022. Metabolic remodeling in takotsubo syndrome. Front. Cardiovasc. Med. 9, 1060070. https://doi.org/10.3389/fcvm.2022.1060070.
Xu, M., Guan, Q., Liu, T., Huang, Y., Pan, C., Luo, L., Tang, W., Xu, J., Huang, H., Xiao, L., Liu, K., Chen, J., 2024. In-hospital adverse events of pheochromocytoma-induced takotsubo syndrome: a literature review and cluster analysis of 172 cases. Rev. Cardiovasc. Med. 25, 216. https://doi.org/10.31083/j.rcm2506216.
Yoganathan, T., Perez-Liva, M., Balvay, D., Le Gall, M., Lallemand, A., Certain, A., Autret, G., Mokrani, Y., Guillonneau, F., Bruce, J., Nguyen, V., Gencer, U., Schmitt, A., Lager, F., Guilbert, T., Bruneval, P., Vilar, J., Maissa, N., Mousseaux, E., Viel, T., Renault, G., Kachenoura, N., Tavitian, B., 2023. Acute stress induces long-term metabolic, functional, and structural remodeling of the heart. Nat. Commun. 14, 3835. https://doi.org/10.1038/s41467-023-39590-3.
Zulfaj, E., Nejat, A., Espinosa, A.S., Hussain, S., Haamid, A., Soliman, A.E., Kakaei, Y., Jha, A., Redfors, B., Omerovic, E., 2024. Development of a small animal model replicating core characteristics of takotsubo syndrome in humans. Eur. Heart J. Open 4, oeae048. https://doi.org/10.1093/ehjopen/oeae048.